



**ROLL-DAMPING DERIVATIVE CALCULATIONS
FOR SPINNING SHARP AND BLUNT CONES
IN SUPERSONIC AND HYPERSONIC FLOW**

**Arloe W. Mayne, Jr.
ARO, Inc., a Sverdrup Corporation Company**

**VON KÁRMÁN GAS DYNAMICS FACILITY
ARNOLD ENGINEERING DEVELOPMENT CENTER
AIR FORCE SYSTEMS COMMAND
ARNOLD AIR FORCE STATION, TENNESSEE 37389**

February 1979

Final Report for Period October 1, 1977 — August 31, 1978

Approved for public release; distribution unlimited.

Prepared for

**ARNOLD ENGINEERING DEVELOPMENT CENTER/DOTR
ARNOLD AIR FORCE STATION, TENNESSEE 37389**

NOTICES

When U. S. Government drawings, specifications, or other data are used for any purpose other than a definitely related Government procurement operation, the Government thereby incurs no responsibility nor any obligation whatsoever, and the fact that the Government may have formulated, furnished, or in any way supplied the said drawings, specifications, or other data, is not to be regarded by implication or otherwise, or in any manner licensing the holder or any other person or corporation, or conveying any rights or permission to manufacture, use, or sell any patented invention that may in any way be related thereto.

Qualified users may obtain copies of this report from the Defense Documentation Center.

References to named commercial products in this report are not to be considered in any sense as an indorsement of the product by the United States Air Force or the Government.

This report has been reviewed by the Information Office (OI) and is releasable to the National Technical Information Service (NTIS). At NTIS, it will be available to the general public, including foreign nations.

APPROVAL STATEMENT

This report has been reviewed and approved.



ELTON R. THOMPSON
Project Manager, Research Division
Directorate of Test Engineering

Approved for publication:

FOR THE COMMANDER



ROBERT W. CROSSLEY, Lt Colonel, USAF
Acting Director of Test Engineering
Deputy for Operations

UNCLASSIFIED

REPORT DOCUMENTATION PAGE		READ INSTRUCTIONS BEFORE COMPLETING FORM
1 REPORT NUMBER AEDC-TR-78-64	2 GOVT ACCESSION NO.	3 RECIPIENT'S CATALOG NUMBER
4 TITLE (and Subtitle) ROLL-DAMPING DERIVATIVE CALCULATIONS FOR SPINNING SHARP AND BLUNT CONES IN SUPERSONIC AND HYPERSONIC FLOW		5 TYPE OF REPORT & PERIOD COVERED Final Report - October 1, 1977 - August 31, 1978
		6 PERFORMING ORG REPORT NUMBER
7 AUTHOR(s) Arloe W. Mayne, Jr., ARO, Inc., a Sverdrup Corporation Company		8 CONTRACT OR GRANT NUMBER(s)
9 PERFORMING ORGANIZATION NAME AND ADDRESS Arnold Engineering Development Center/DOTR Air Force Systems Command Arnold Air Force Station, Tennessee 37389		10 PROGRAM ELEMENT, PROJECT, TASK AREA & WORK UNIT NUMBERS Program Element 65807F
11 CONTROLLING OFFICE NAME AND ADDRESS Arnold Engineering Development Center/DOS Air Force Systems Command Arnold Air Force Station, Tennessee 37389		12 REPORT DATE February 1979
		13 NUMBER OF PAGES 23
14 MONITORING AGENCY NAME & ADDRESS (if different from Controlling Office)		15 SECURITY CLASS (of this report) UNCLASSIFIED
		15a DECLASSIFICATION/DOWNGRADING SCHEDULE N/A
16 DISTRIBUTION STATEMENT (of this Report) Approved for public release; distribution unlimited.		
17 DISTRIBUTION STATEMENT (of the abstract entered in Block 20, if different from Report)		
18 SUPPLEMENTARY NOTES Available in DDC		
19 KEY WORDS (Continue on reverse side if necessary and identify by block number) conical bodies roll computations blunt bodies supersonic flow sharp bodies hypersonic flow spinning (motion) boundary layer damping equations		
20 ABSTRACT (Continue on reverse side if necessary and identify by block number) The boundary-layer equations in a Crocco variables form have been numerically solved for flow over spinning sharp and blunt cones at zero incidence to supersonic and hypersonic streams. Both laminar and turbulent flows have been treated, and for the blunt cases swallowing of the inviscid entropy layer by the boundary layer has been considered. The item of primary interest is roll damping, and results of a parametric study involving Mach number, Reynolds number, cone angle, and bluntness ratio are presented. Limited comparisons with experimental data and another method of computation are also presented.		

UNCLASSIFIED

PREFACE

The work reported herein was conducted by the Arnold Engineering Development Center (AEDC), Air Force Systems Command (AFSC), under Program Element 65807F. The results of the research presented were obtained by ARO, Inc. (a Sverdrup Corporation Company), operating contractor for the AEDC, AFSC, Arnold Air Force Station, Tennessee, under ARO Project Number V32A-P1A. The manuscript was submitted for publication on September 15, 1978.

Acknowledgement and appreciation is extended to the following persons who aided in the work reported herein: Mrs. B. M. Majors, ARO, Inc., who performed the majority of the calculations used in the report; Dr. J. C. Adams, ARO, Inc., who provided the solution made using the method of Ref. 2; and to Mr. E. O. Marchand, formerly of ARO, Inc., whose method was used for computing the inviscid flow for the sharp cases.

CONTENTS

	<u>Page</u>
1.0 INTRODUCTION	5
2.0 THEORETICAL METHOD	6
3.0 RESULTS OF CALCULATIONS	
3.1 Comparisons with Other Data	9
3.2 Body Geometry and Free-Stream Conditions	11
3.3 Wall Temperature and Spin-Rate Effects	12
3.4 Reynolds Number Scaling	12
3.5 Parametric Study Results	14
4.0 SUMMARY AND CONCLUSIONS	19
REFERENCES	21

ILLUSTRATIONS

Figure

1. Inviscid Entropy Layer Swallowing by Boundary Layer	8
2. Measured and Computed Roll-Damping Derivative versus Bluntness Ratio for a 10-deg Cone in a Mach 14.25 Flow	10
3. Roll-Damping Derivative versus Bluntness Ratio for a 7.5-deg Blunt Cone in a Mach 8 Stream under Laminar and Turbulent Flow Conditions	13
4. Roll-Damping Derivative, Scaled by Reynolds Number to a Power, versus Bluntness Ratio	14
5. Roll-Damping Derivative versus Bluntness for 5.0-, 7.5-, and 10.0-deg Cones in Mach 6 Flow	15
6. Roll-Damping Derivative versus Bluntness for 5.0-, 7.5-, and 10.0-deg Cones in Mach 8 Flow	16
7. Roll-Damping Derivative versus Bluntness for 5.0-, 7.5-, and 10.0-deg Cones in Mach 10 Flow	17

<u>Figure</u>	<u>Page</u>
8. Roll-Damping Derivative versus Bluntness for 5.0-, 7.5-, and 10.0-deg Cones in Mach 14 Flow	18
9. Roll-Damping Derivative versus Bluntness for 5.0-, 7.5-, and 10.0-deg Cones in Mach 22 Flow at Altitudes of 50, 80, and 120 kft	20
10. Roll-Damping Derivative versus Bluntness for 5.0-, 7.5-, and 10.0-deg Cones in Mach 22 Flow at 200-kft Altitude with Laminar Flow	21
NOMENCLATURE	23

1.0 INTRODUCTION

The computation of reentry vehicle motion requires knowledge of a number of aerodynamic coefficients; these may come from correlations of experimental data or from theoretical calculations. As more accurate trajectory predictions are required, more accurate aerodynamic coefficients must be obtained. Because many vehicles are caused to spin during entry into the atmosphere, the effects of viscous aerodynamic damping on the spin rate must be known in order to predict the performance of the vehicles. A knowledge of roll-damping effects is also valuable for the prediction, corroboration, and evaluation of wind tunnel test data.

Approximate methods, such as those used in Ref. 1, have been applied in the past to compute roll-damping data, and such methods do provide reasonable results when properly applied. Recently, more exact methods, such as in Ref. 2 and those used in the present study, have become available for computation of the viscous flow over spinning bodies.

It is the purpose of this report to present a method which has been developed for the computation of the boundary-layer flow over spinning sharp and blunt cones in supersonic and hypersonic streams, and to present the results of a parametric study of the effects of Mach number, Reynolds number, cone angle, and bluntness ratio on the roll-damping derivative for a family of sharp and blunt cones at zero angle of attack. Both laminar and turbulent boundary layers have been considered, and for the blunt cases the effects of swallowing of the inviscid entropy layer by the boundary layer were included in the analysis. Some investigations were also made of the effects of vehicle wall temperature and roll rate, and Reynolds number scaling of the roll-damping derivative was examined. Conditions were considered which are typical of both wind tunnel and free-flight situations, and limited comparisons were made with experimental data and results of other computations.

2.0 THEORETICAL METHOD

The treatment of the boundary-layer equations used in this investigation evolved from a study of three-dimensional boundary-layer flows (Refs. 3 and 4). This resulted from the fact that the three-dimensional boundary-layer equations include the lateral momentum equation and contain the cross-flow velocity terms needed to treat the spinning body case, although they are much more general than needed in the axisymmetric flow situations considered in this investigation.

The compressible boundary-layer equations, including the cross-flow velocity terms, were cast into a normalized Crocco-variables form and solved using an implicit finite difference technique developed by Taylor series truncation. The Crocco transformation is accomplished by letting the coordinate normal to the body surface be the normalized longitudinal velocity component. This yields the convenient limits of zero and unity for the normal coordinate. The velocity component normal to the body surface is eliminated from the governing equations by combining the longitudinal momentum equation with each of the continuity, lateral momentum, and energy equations. This decreases the number of partial differential equations to be solved from four to three. As a part of the transformation, a form of the longitudinal component of the shearing stress becomes the dependent variable associated with the transformed longitudinal momentum/continuity equation. The energy equation is cast in terms of the total enthalpy, and the gas under consideration has been treated as both thermally and calorically perfect, being air for all of the cases considered. The specific forms of the governing equations, transport laws, difference equations, etc., are not given herein, but are the axisymmetric flow forms of those given in Refs. 3 and 4.

For turbulent boundary-layer flow, the viscosity and Prandtl number in the governing equations were treated as effective transport parameters, and an eddy-exchange coefficient treatment of the turbulent transport

parameters was used. The turbulent viscosity was specified using the mixing-length, invariant turbulence model as applied by Hunt, Bushnell, and Beckwith (Ref. 5), with the mixing length obtained using a two-layer model with exponential damping near the wall as recommended by van Driest (Ref. 6). The variation of the mixing length was obtained from the recommendations of Patankar and Spalding (Ref. 7). Transition from laminar to turbulent flow was treated by the use of the streamwise intermittency factor determined by Dhawan and Narashima (Ref. 8), with the beginning and end of transition being fixed at $x/r_n = 1.5$ and 2.0 , respectively, for the blunt cases and at $x = 0.1$ ft and 0.15 ft, respectively, for the sharp cases. A turbulent Prandtl number of 0.9 and a laminar Prandtl number of 0.7 were assumed in this work.

The governing equations degenerated to two-point boundary-value problems at a sharp tip or stagnation point, and formed a parabolic system which could be solved by marching down the remainder of the body. The boundary conditions required were generally the values of the dependent variables on the body surface and at the outer edge of the boundary-layer, together with the longitudinal derivatives of the outer-edge conditions. Wall boundary conditions were provided by the no-slip condition and a specified surface temperature, together with the inviscid surface pressure, which was assumed constant with respect to the direction normal to the surface, the standard boundary-layer assumption.

For the sharp cases, the outer-edge boundary conditions were taken as the inviscid body surface conditions. For the blunt cases, the outer-edge boundary conditions were determined from inviscid flow data, based on consideration of the swallowing by the boundary layer of the inviscid entropy layer. Entropy swallowing is based on a mass-flow balance between the boundary layer at a given location and the free stream in order to find the shock angle crossed by the outer-edge flow at the location of interest. This is shown in Fig. 1. Inviscid shock shape and surface pressure data were obtained using the blunt body treatment of Ref. 9 and the method of characteristics treatment of Ref. 10.

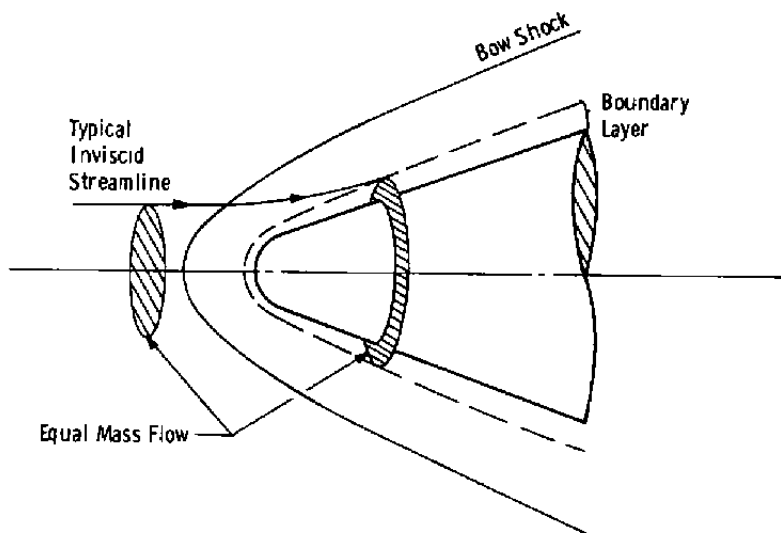


Figure 1. Inviscid entropy layer swallowing by boundary layer.

This method of solution of the governing partial-different equations involved replacing them by a set of consistent, linearized, algebraic equations. The resulting set was of tridiagonal form and could be solved by means of the well-known algorithm available for such cases. The solution required iteration to remove the assumptions made in the linearization, and cases which considered entropy swallowing involved an outer iteration concerned with the determination of consistent outer-edge boundary conditions.

3.0 RESULTS OF CALCULATIONS

In this section, results of calculations made using the method described in the previous section are presented. Comparisons are made with experimental data and results from another method of calculation. These comparisons tend to validate the method developed in this investigation. Results of an examination of the effects of vehicle wall temperature and spin rate on the roll-damping derivative are presented, and some considerations of Reynolds number scaling are also discussed.

The bulk of the results obtained in this investigation are presented as a series of figures which give the behavior of the roll-damping derivative of a sphere-cone as a function of body bluntness (ratio of nose radius to base radius) for a range of Mach numbers, Reynolds number, and cone angles. Results are shown for both laminar and turbulent boundary-layer flows for those cases pertinent to wind tunnel flows, namely Mach numbers of 6, 8, 10, and 14. For the Mach 22 data which is representative of atmospheric entry conditions, laminar flow results are given for altitudes of 200, 120, and 80 kft, and turbulent flow results are given for altitudes of 120, 80, and 50 kft.

All of the calculations made in this investigation were performed on an IBM 370/165 digital computer.

3.1 COMPARISONS WITH OTHER DATA

To validate the method used, results of calculations made using the present method have been compared with experimental data and with results from another method of computation. Figure 2 shows the roll-damping derivative versus nose bluntness ratio for laminar flow over a rotating 10-deg blunt cone in a Mach 14.25 flow. Results from boundary-layer calculations are compared with experimental data reported in Ref. 1. The agreement between the measurements and the calculations is reasonably good, with the computed results being from one to five percent above the measurements, depending on the bluntness ratio. It is difficult to make a statement about the quantitative agreement between the two sets of data because of a lack of information about the uncertainty in the experimental data. It is known that accurate experimental data of this nature are hard to obtain because of the large bearing-damping corrections which must usually be made. The present method was further validated by solving the sharp-cone case of Fig. 2 using the method of Ref. 2. The results obtained using that method agreed to within two percent with the lateral skin-friction coefficient obtained using the present method.

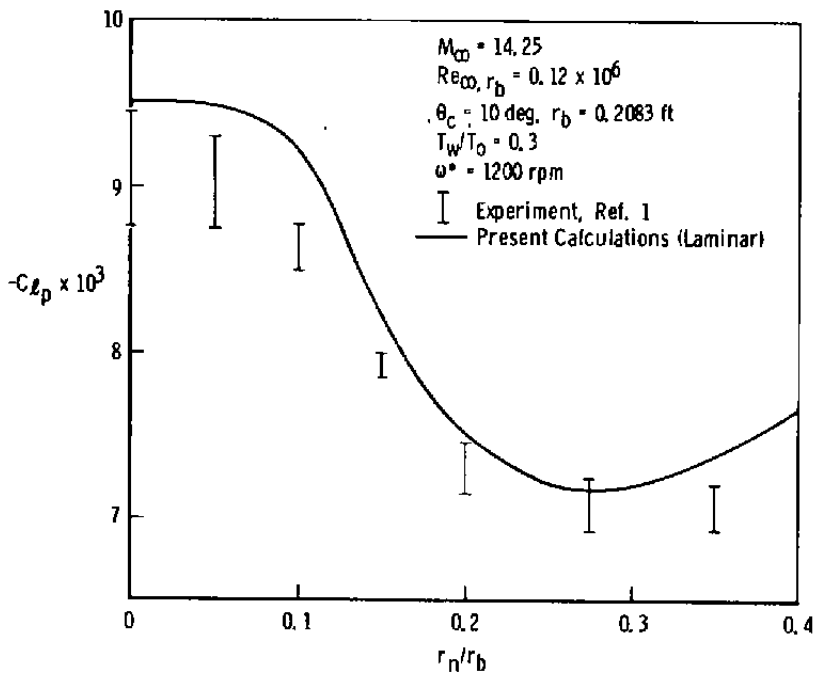


Figure 2. Measured and computed roll-damping derivative versus bluntness ratio for a 10-deg cone in a Mach 14.25 flow.

In general, the calculations made in this investigation used the Sutherland viscosity-temperature relationship; however, for the cases shown in Fig. 2, the Sutherland law was used only for temperatures above 200°R , with a linear temperature-viscosity relationship being used for temperatures below 200°R . This was necessitated by the fact that the free-stream static temperature for these cases was approximately 50°R , and the viscosity-temperature relationship is not well modeled at this low temperature by the Sutherland Law. Since the free-stream conditions are used as reference conditions in the theoretical treatment of the problem it is necessary that the free-stream viscosity be properly computed even though such low temperatures do not actually exist within the boundary layer. Use of the Sutherland viscosity law exclusively for the cases of Fig. 2 yielded a roll-damping derivative curve approximately thirteen percent above that shown. For the remainder of the calculations made in this investigation, the free-stream static temperature was 100°R or higher, and for these cases only the Sutherland

viscosity was used. The estimated variation in the roll-damping derivative is less than three percent when ignoring the linear portion of the viscosity-temperature law for these cases.

One further point to be made in examining Fig. 2 is the manner in which the blunt cone results approach the sharp cone ($r_n/r_b = 0$) value as the bluntness ratio is reduced. Physically, this is a natural occurrence, but computationally it occurs only because of the inclusion of entropy swallowing in the analysis. In fact, if entropy swallowing were neglected, the blunt-cone results would approach a value approximately fifteen percent below the sharp-cone value as the bluntness is reduced to zero. Since the sharp-cone results were obtained using an entirely different code than for the blunt cone, the consistency between the sharp-cone value and the results obtained including entropy swallowing in the blunt-body analysis demonstrates a consistency between the two codes and the necessity for including entropy swallowing in the computations.

3.2 BODY GEOMETRY AND FREE-STREAM CONDITIONS

The remainder of the results to be presented are roll-damping derivative data on a family of sharp and blunt cones of semi-vertex angles of 5.0, 7.5, and 10.0 deg. For a given cone angle, the base radius was held constant, and the nose radius varied to give various bluntness ratios. Base radii of 4.0, 4.5, and 5.0 in. were used for the 5.0-, 7.5-, and 10.0-deg cones, respectively. Calculations were performed for nose-to-base radius ratios of 0.0, 0.05, 0.15, and 0.25 in each case.

For the Mach 6, 8, 10, and 14 cases, a free-stream static temperature of 100°R and unit Reynolds numbers of 0.5×10^6 and 3.0×10^6 per ft were considered as being typical of wind tunnel conditions. Standard values of wall temperature of 600°R and spin rate of 500 rpm were used. Laminar and turbulent flow were considered in all of these cases.

For the free-flight cases, a Mach number of 22 was used together with a wall temperature of 2000°R and a spin rate of 100 rpm. The same geometries as previously mentioned were treated. Cases were run for laminar flow at 200-, 120-, and 80-kft altitudes, and for turbulent flow at altitudes of 120, 80, and 50 kft.

3.3 WALL TEMPERATURE AND SPIN-RATE EFFECTS

Variations of wall temperature and spin rate from that of Section 3.2 were considered, and the results are presented in this section.

The Mach 8, $\theta_c = 7.5\text{-deg}$, $r_n/r_b = 0.15$ case was run with spin rates of 100, 500, and 1,000 rpm, and with wall temperatures of 600°R and an adiabatic wall condition. These cases were run at unit Reynolds numbers of 0.5×10^6 and $3.0 \times 10^6/\text{ft}$, considering both laminar and turbulent boundary layers.

For these various conditions, the net effect of the spin rate variation on the roll-damping derivative was less than one percent for the range of spin rate considered, holding other parameters fixed.

The roll-damping derivative was substantially increased by changing the wall temperature from 600°R to an adiabatic wall condition (a wall temperature in the vicinity of 1200°R). For the lower Reynolds number laminar and turbulent cases and the higher Reynolds number laminar cases, this increase was approximately ten percent. For the higher Reynolds number turbulent cases, the increase caused by the increase in wall temperature was approximately twenty percent.

3.4 REYNOLDS NUMBER SCALING

Typical results of the parametric study of the effects of Mach number, Reynolds number, cone angle, and bluntness ratio on the roll-

damping derivative of blunt cones are shown in Fig. 3. This figure shows the roll-damping derivative versus nose bluntness ratio for both laminar and turbulent flow on a 7.5-deg cone in a Mach 8 free stream. Because of (a) the inclusion of the cross-flow terms in the governing equations, (b) the consideration of entropy layer swallowing by the boundary layer, and (c) the consideration of turbulent flow, the governing equations considered in this study do not, strictly speaking, have similarity solutions which allow casting the results in a Reynolds number independent form. Evidently, however, the effects of (a) and (b) are not strong in the laminar cases shown in Fig. 3, and the application of conventional Reynolds number scaling yields the essentially Reynolds number independent data shown in the upper part of Fig. 4. Heuristically

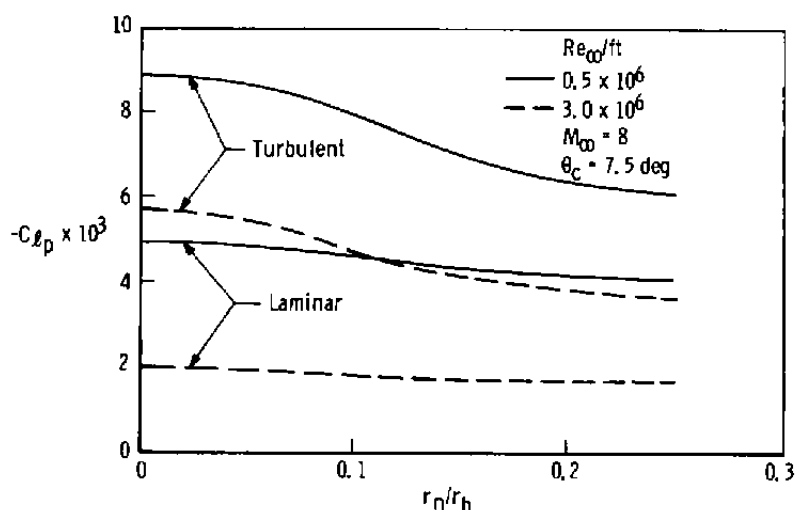


Figure 3. Roll-damping derivative versus bluntness ratio for a 7.5-deg blunt cone in a Mach 8 stream under laminar and turbulent flow conditions.

treating the turbulent flow data of Fig. 3 in a similar manner yields the result shown in the lower part of Fig. 4, where the 0.27 power on the Reynolds number was determined empirically as a value which reasonably collapsed the data. Although the remainder of the data to be presented in this report will be in the format of Fig. 3, having the data in the form given in Fig. 4 could make its use more convenient in motion analysis.

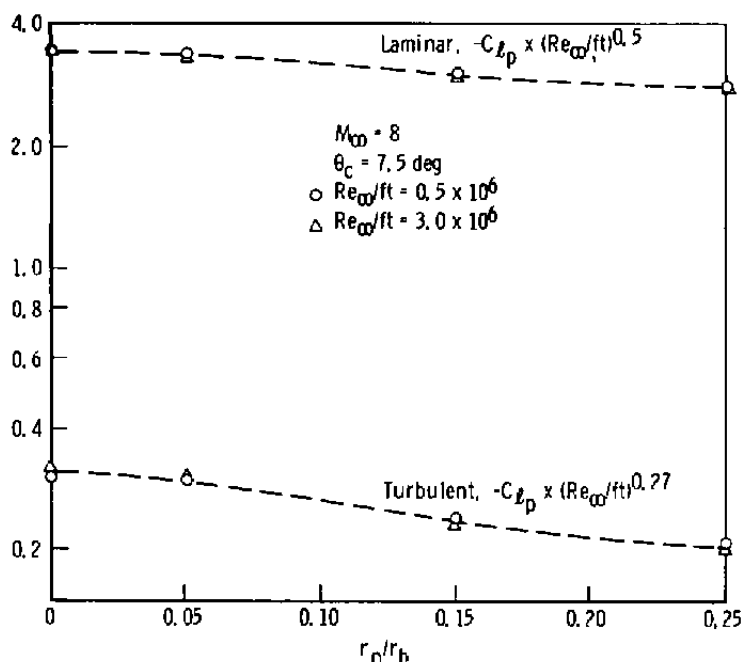


Figure 4. Roll-damping derivative, scaled by Reynolds number to a power, versus bluntness ratio.

3.5 PARAMETRIC STUDY RESULTS

The bulk of the results obtained in this investigation are presented in Figs. 5 through 10. These figures give the variation of the roll-damping derivative of a sphere-cone as a function of body bluntness. Each figure has a separate set of curves for cone angles of 5.0, 7.5, and 10.0 deg.

Figures 5 through 8 present data for free-stream Mach numbers of 6, 8, 10, and 14, respectively. Each Mach number-cone angle combination has both laminar and turbulent flow results for free-stream unit Reynolds numbers of 0.5×10^6 and $3.0 \times 10^6/\text{ft}$. Generally speaking, the negative of the roll-damping derivative decreases with increasing bluntness. The variation between the sharp and the 0.25 bluntness values is generally greater for the turbulent cases than the laminar, i.e., the effect of bluntness is

greater for the turbulent cases. Also, for the range of bluntness considered, the effect of bluntness generally increases with increasing free-stream Mach number.

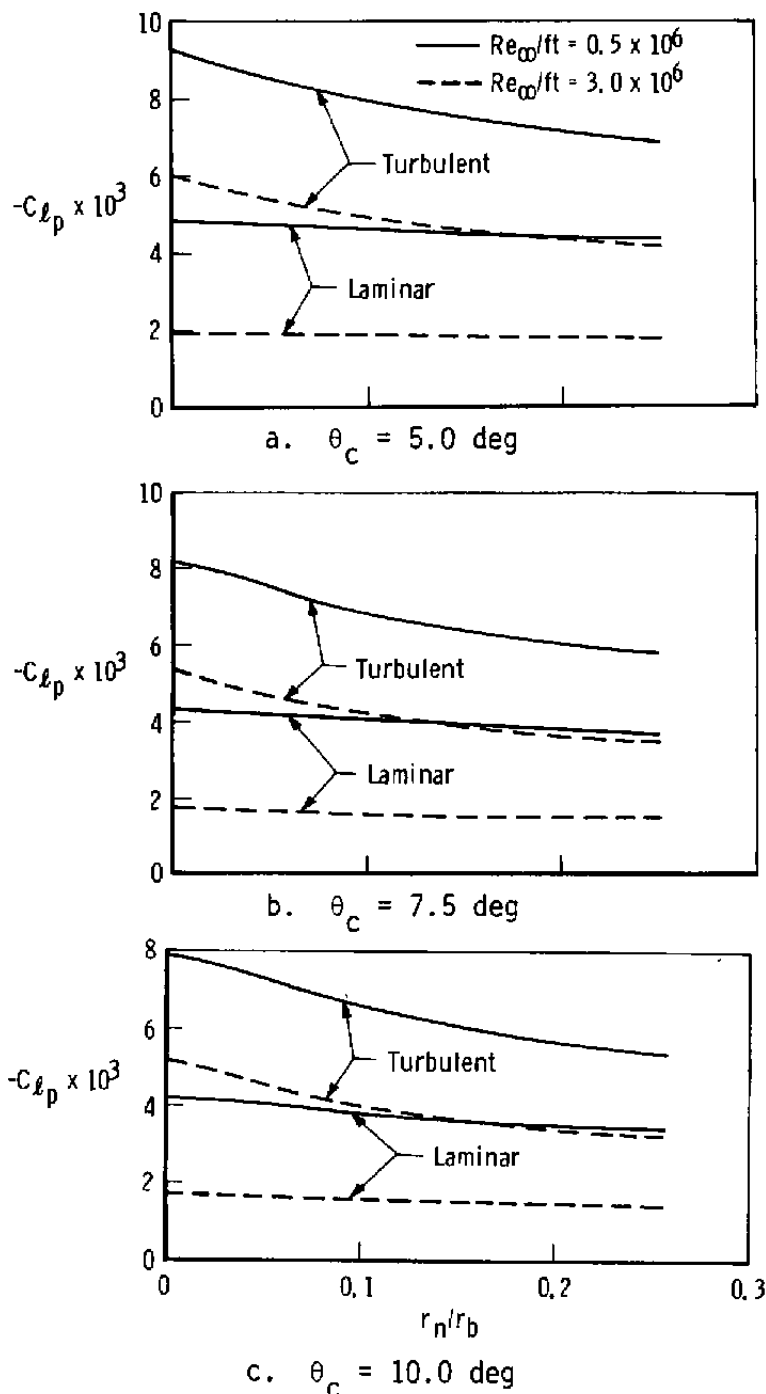


Figure 5. Roll-damping derivative versus bluntness for 5.0-, 7.5-, and 10.0-deg cones in Mach 6 flow.

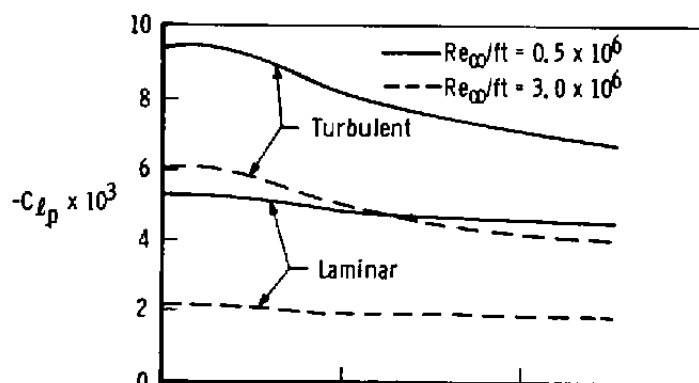
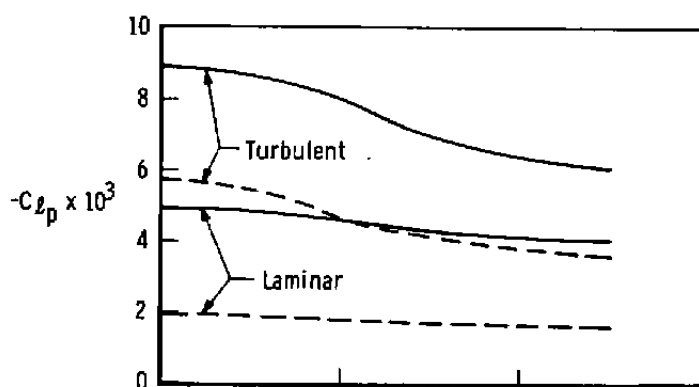
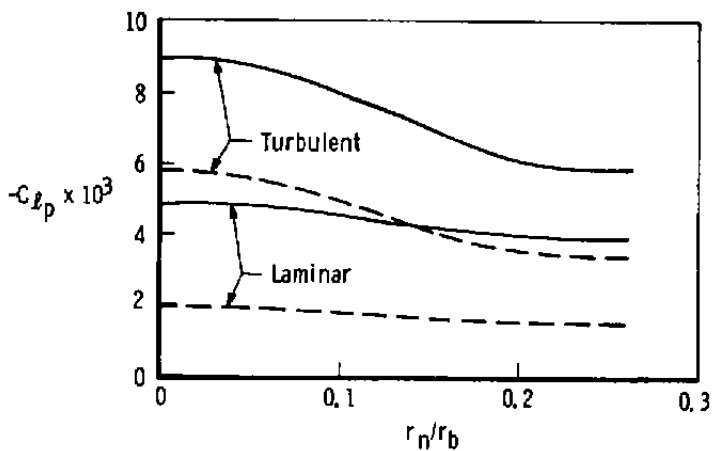
a. $\theta_c = 5.0$ degb. $\theta_c = 7.5$ degc. $\theta_c = 10.0$ deg

Figure 6. Roll-damping derivative versus bluntness for 5.0-, 7.5-, and 10.0-deg cones in Mach 8 flow.

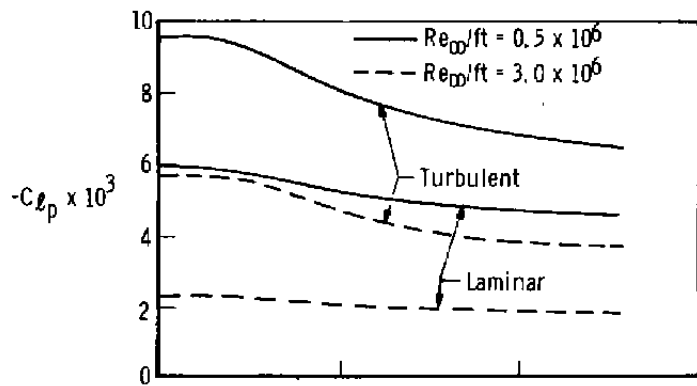
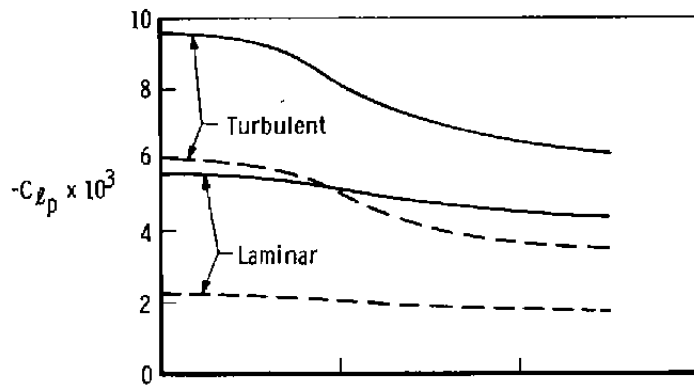
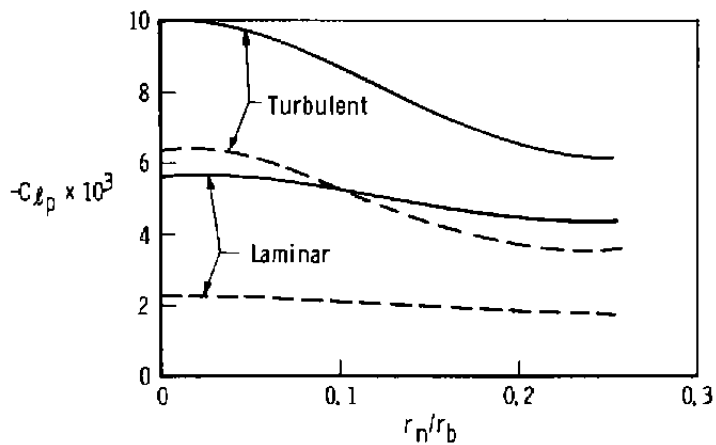
a. $\theta_c = 5.0$ degb. $\theta_c = 7.5$ degc. $\theta_c = 10.0$ deg

Figure 7. Roll-damping derivative versus bluntness for 5.0-, 7.5-, and 10.0-deg cones in Mach 10 flow.

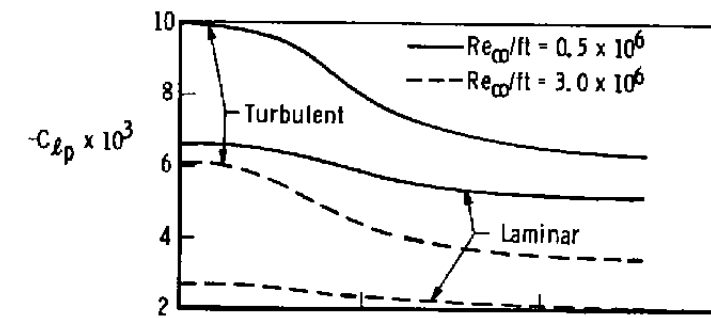
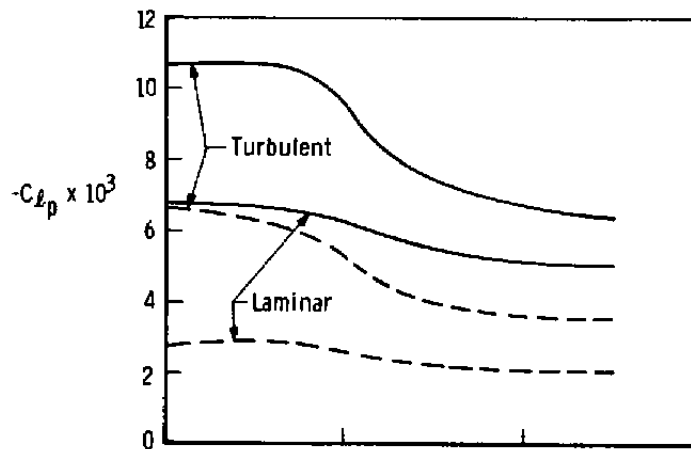
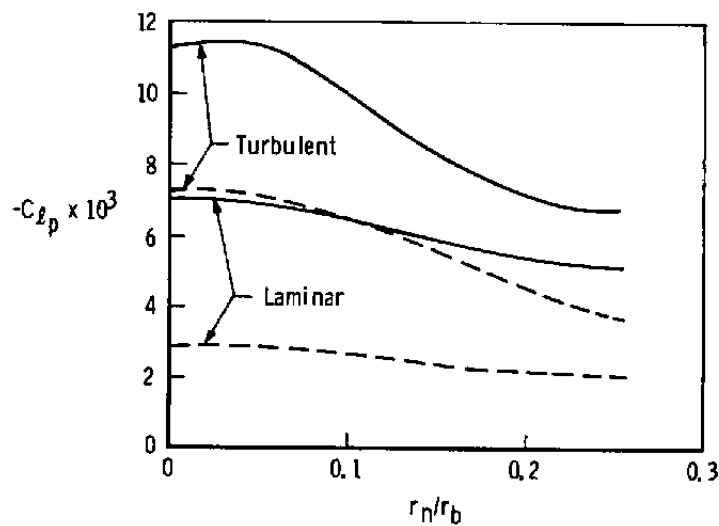
a. $\theta_c = 5.0$ degb. $\theta_c = 7.5$ degc. $\theta_c = 10.0$ deg

Figure 8. Roll-damping derivative versus bluntness for 5.0-, 7.5-, and 10.0-deg cones in Mach 14 flow.

Figures 9 and 10 present the roll-damping derivative results obtained for the Mach 22 flight conditions considered. For these cases, the free-stream Reynolds number and static temperature depend upon the altitude for each specific case. The free-stream unit Reynolds number varies from approximately 26 million per ft at 50-kft altitude to 36 thousand per ft at 200-kft altitude, and the mean free-stream temperature is approximately 420°R. Figure 9 presents the results for the 50-, 80-, and 120-kft altitude cases, where both laminar and turbulent results are given for the two higher altitudes, and only turbulent results are given for the lowest altitude case. In Fig. 10, laminar flow results are presented for the 200-kft altitude cases.

The primary purpose of Figs. 5 through 10 is to provide data for use in the analysis of the motion of spinning reentry vehicles in the wind tunnel and in free flight. It is hoped that the range of parameters considered is adequate for this purpose.

4.0 SUMMARY AND CONCLUSIONS

A theoretical method of computing the boundary-layer flow over spinning sharp and blunt cones in supersonic and hypersonic flow has been described. The method was validated by being shown to give good agreement with experimental data and another method of computation. Wall temperature and spin-rate effects on roll-damping derivative data were examined, and a method of casting the roll-damping derivative data into a Reynolds number independent form was presented.

The bulk of the data presented were the results of a parametric study of the effects on the roll-damping derivative of Mach number, Reynolds number, cone angle, and bluntness ratio. The results were for a range of the parameters which should allow their application to the analysis of the motion of spinning cones in both wind tunnel and flight situations.

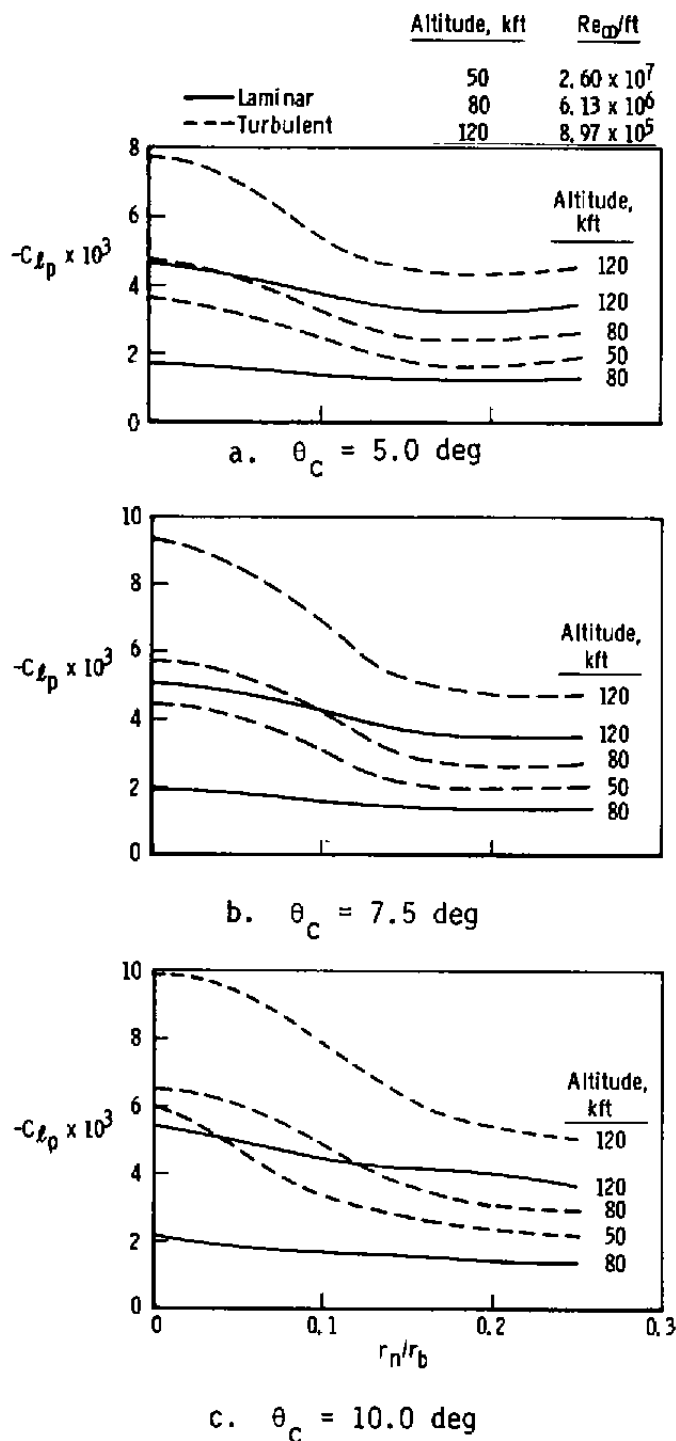


Figure 9. Roll-damping derivative versus bluntness for 5.0-, 7.5-, and 10.0-deg cones in Mach 22 flow at altitudes of 50, 80, and 120 kft.

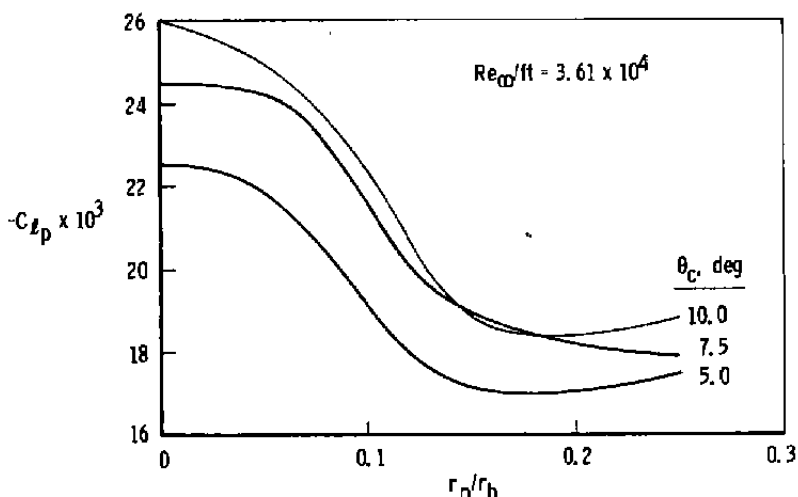


Figure 10. Roll-damping derivative versus bluntness for 5.0-, 7.5-, and 10.0-deg cones in Mach 22 flow at 200-kft altitude with laminar flow.

REFERENCES

1. Walchner, O. "Laminar Hypersonic Roll Damping Derivatives for a 10-deg Cone." AIAA Journal, Vol. 7, No. 2, February 1969, pp. 342-343.
2. Lin, T. C. and Rubin, S. G. "Viscous Flow over Spinning Cones at Angle of Attack." AIAA Journal, Vol. 12, No. 7, July 1974, pp. 975-985.
3. Mayne, A. W., Jr. "Analysis of Laminar Boundary Layers on Right Circular Cones at Angle of Attack, Including Streamline-Swallowing Effects." AEDC-TR-72-134 (AD750130), October 1972.
4. Mayne, A. W., Jr. "Calculation of the Boundary-Layer Flow in the Windward Symmetry Plane of a Spherically Blunted Axisymmetric Body at Angle of Attack, Including Streamline-Swallowing Effects." AEDC-TR-73-166 (AD768340), October 1973.
5. Hunt, J. L., Bushnell, D. M., and Beckwith, I. E. "The Compressible Turbulent Boundary Layer on a Blunt Slab with and without Leading-Edge Blowing." NASA-TN-D-6203, March 1971.
6. van Driest, E. R. "On Turbulent Flow Near a Wall." J. Aero. Sci., Vol. 23, No. 3, March 1956, pp. 1007-1011, 1036.

7. Patankar, S. V. and Spalding, D. B. Heat and Mass Transfer in Boundary Layers. CRC Press, Cleveland, 1968.
8. Dhawan, S. and Narasimha, R. "Some Properties of Boundary-Layer Flow during the Transition from Laminar to Turbulent Motion." Journal of Fluid Mechanics, Vol. 3, No. 4, April 1958, pp. 418-436.
9. Aungier, R. H. "A Computational Method for Exact, Direct, and Unified Solutions for Axisymmetric Flow Over Blunt Bodies of Arbitrary Shape (Program BLUNT)." AFWL-TR-70-16, July 1970.
10. Inouye, M., Rakich, J. V., and Lomax, H. "A Description of Numerical Methods and Computer Programs for Two-Dimensional and Axisymmetric Supersonic Flow over Blunt-Nosed and Flared Bodies." NASA TN D-2970, August 1965.

NOMENCLATURE

A	Base area
C_{ℓ_p}	Roll-damping derivative, $\partial \left(\frac{L}{q_\infty A d} \right) / \partial \left(\frac{p r_b}{U_\infty} \right)$
d	Base diameter
L	Rolling moment
M_∞	Free-stream Mach number
p	Roll rate, radians/sec
q_∞	Free-stream dynamic pressure
Re_∞/ft	Free-stream unit Reynolds number, 1/ft
Re_∞, r_b	Free-stream Reynolds number based on base radius
r_b	Base radius
r_n	Nose radius
T_w/T_o	Ratio of surface temperature to free-stream total temperature
U_∞	Free-stream velocity
x	Surface distance from stagnation point or sharp tip
θ_c	Cone angle (semi-vertex angle)
ω^*	Roll rate, rev/min